ISSN 2321-807X
Volume 13 Number3
Journal of Advances in chemistry

THE STRUCTURAL, MORPHOLOGICAL AND OPTICAL STUDY OF PURE AND W-DOPED TiO2 NANO PARTICLES AND ITS APPLICATION TO ANTIMICROBIAL ACTIVITY

K. Manikandan[1*], A. Jafar Ahamed[2], N. Jayakumar[3]
[1] Department of Chemistry, Velalar College of Engineering and Technology (Autonomous), Erode-638 012, India.
[2] PG and Research Department of Chemistry, Jamal Mohamed College (Autonomous), Trichy-620 020, India.
[3] Department of Chemistry, Sri Vasavi College, Erode – 638 316, India.

ABSTRACT

In this research work, the effect of tungsten-doping on the crystal structure, morphology and antimicrobial of titanium dioxide nanoparticles were studied. The pure and different weight %

of tungsten doped TiO_2 nanoparticles were synthesized by sol-gel method and calcinated at 600° C for 5 h. The synthesised products have been characterized by X-ray Diffraction studies (XRD), Field Emission Scanning Electron Microscopy (FESEM), Energy Dispersive X-ray analysis (EDXA), Ultraviolet-Visible Diffuse Reflectance Spectroscope (UV-Vis), Photoluminescence Spectra (PL), High Resolution Transmission Spectroscopy (HRTEM) and Fourier Transform Infra Red Spectroscopy (FT-IR). XRD pattern of pure TiO_2 and 1 wt % W-doped TiO_2 nanoparticles confirms the anatase structure and increase in the W-doping changes the phase of TiO_2 to rutile. Average crystallite size of synthesized nanoparticles was determined using the Debye-Scherrer formula. The crystallite size obtained for pure TiO_2 is 37 nm and W-doped TiO_2 is 28 nm, 34 nm and 33 nm. The FESEM images show the agglomerated particles of spherical-like morphology. Optical property and direct bandgap of pure and W-doped TiO_2 nanoparticles also further characterised by UV–Vis Spectroscopy. The images of HRTEM clearly confirm that particles present in the W-doped TiO_2 powdered sample is nanosized particles. The Kirby Bauer Agar Well Diffusion Assay method was employed to explore antimicrobial activity of nanosized pure and W-doped TiO_2 colloidal suspension against the test microorganisms two Gram positive bacteria (*Staphylococcus aureus, Bacillus subtilis*), two Gram negative Bacteria (*Escherichia coli, Pseudomonas aeruginosa*) and two fungi (*Candida albicans, Aspergillus niger*). It shows that the W-doped TiO_2 nanoparticles inhibited the multiplication and growth of the above mentioned test bacteria and fungi. Antimicrobial activity was found against all tested microorganisms which confirmed that W-doped TiO_2 nanoparticles possess high antimicrobial activity compared to pure TiO_2 nanoparticles.

Keywords: Nanoparticles, Sol–gel method, XRD, HRTEM, Antimicrobial activity.

*Corresponding author. Tel:+91 4242244201; FAX:+914242244205.

Email address: chemmani03@gmail.com (K.Manikandan).

. INTRODUCTION

Titanium dioxide is used as an eco friendly photo catalyst. It is an inexpensive, easily available, nontoxicity and chemically stable one. However, TiO_2 is used other than photocatalyst and this is used in catalyst support, photoconductors, solar cells, gas sensors, coatings etc. Now the scientist are focused in antimicrobial activity of TiO_2 due to its rapid recombination of photo activated electrons and positive holes. Titanium dioxide present in three different crystalline phases: rutile, anatase, and brookite. Out of these three phases, Rutile phase is stable one compared to other two phases are in metastable. Anatase and rutile systems have tetragonal unit cells. The rutile phase possesses two TiO_2 molecules per unit cell having lattice constant a=4.5937A° and c=2.9587 A° and the anatase phase has four TiO_2 molecules per unit cell having lattice constant a=3.7842 A° and c=9.5146 A°. Generally, the temperature of TiO_2 nano crystal is increased to above 450° C [1, 2] phase has been changed from anatase to rutile structure. Anatase and rutile phases of TiO_2 nanocrystals are the two important photoactive polymorphic phases with the band-gap energy of 3.20 eV and 3.02 eV respectively [3]. Band gap value of the anatase phase is larger than that of the rutile phase, so the rutile phase properties are slightly better than the anatase phase properties in semiconducting performance [4]. In recent years, researcher's showed interest on the antimicrobial activity of doping of titanium dioxide with transition metals like tungsten, cobalt etc.

In this present study, synthesis of W-doped TiO_2 nanoranged particles by sol-gel method is to study the highest possible antimicrobial activity and it can be compared with pure TiO_2 also prepared by solgel method. There are several methods such as sol-precipitation [5], ion-impregnation [6], hydrothermal synthesis [7], sol-gel synthesis [8] to available for obtain homogeneous doping of W in TiO_2. But, Sol-gel is the most simple and sophisticated method among the various methods for producing nanoparticles. The preparation of thin film W-doped TiO_2 nanoparticles in a colloidal state by sol-gel method which is used in antimicrobial coatings in water filters, leathers, textiles and medical devices. The prepared W-doped TiO_2 nanoparticles were characterised by different techniques like X-ray diffraction (XRD), Field emission scanning electron microscopy (SEM), Energy dispersive X-ray Spectroscopy (EDXA), UV–Visible Diffuse Reflectance Spectroscopy (UV-Vis), Photoluminescence analysis (PL), Fourier Transform Infra Red spectroscopy (FTIR), and High resolution Transmission Electron Microscopy (HRTEM). The Kirby Bauer Agar Well Diffusion Assay method was employed to explore antimicrobial activity of nanosized pure and W-doped TiO_2 colloidal suspension against the test microorganisms two Gram positive bacteria (*Staphylococcus aureus, Bacillus subtilis*), two Gram negative Bacteria (*Escherichia coli, Pseudomonas aeruginosa*) and two fungi (*Candida albicans, Aspergillus niger*). It shows that the W-doped TiO_2

nanoparticles inhibited the multiplication and the growth of the above mentioned test bacteria and fungi. Antimicrobial activity was found against all tested microorganisms at a concentration range of 25 µg, 50 µg, 75 µg and 100 µg of pure TiO_2, 1 wt %,3 wt % and 5 wt % W-doped TiO_2 solutions.

2. EXPERIMENTAL

2.1. Materials

Titanium isopropoxide (Sigma-Aldrich > 97 % pure), sodium tungstate dihydrate (Merk, 98 % pure), ethanol (Hayman (German) 99.99 % pure), hydroxylamine hydrochloride (Sigma-Aldrich 99 % pure) were used as precursor and is used without any further purification. Doubly distilled water was used for the whole synthesis process. Bacterial cultures such as *Staphylococcus aureus*, *Bacillus subtilis, Escherichia coli, Aspergillus niger* and *fungus* cultures such as *Pseudomonas aeruginosa*, *Candida albicans* were obtained from Eumic analytical Lab and Research Institute, Tiruchirappalli. Bacterial strains were maintained on nutrient agar slants (Hi media) at 4^{o} C.

2.1.1Physicochemical characterization

The X-ray diffraction pattern analysis for pure TiO_2 and doped TiO_2 nanoparticles was recorded by Lab X XRD6000 Shimadzu model with Cu-Ka radiation. The structure and morphology of the nanoparticles were investigated by Field Emission Scanning Electron Microscope (FESEM) using FEI Quanta FEG 200-High Resolution Scanning Electron Microscope. The absorption spectra and optical band gap of the TiO_2 and doped TiO_2 nanoparticles samples were measured by using UV-Vis Spectrophotometer (JASCO U-670 Spectrometer) and the alcohol as a solvent. The spectrum was recorded between 200 – 800 nm. A Photoluminescence spectrum was recorded between 370-770 nm and it was carried out by using Horiba Jobnyvon model spectrophotometer and the alcohol is used as a solvent. FTIR absorption spectrum was recorded by JASCOFP8200 spectrophotometer. The particle size and lattice structure of the individual crystal was visualised by using High Resolution Transmission Electron Microscopy JE2100 (JEOL-200KV, LB6 filament) and EDXA analysis was carried out to find the composition of pure and doped TiO_2 samples by using the detector attached with the same instrument.

2.2. Synthesis of pure TiO_2 and W-doped TiO_2 nanoparticles

Pure titanium dioxide nanoparticles and 1 wt %, 3 wt % and 5 wt % W-doped TiO_2 nanoparticles were prepared by sol gel method [9]. For the preparation of TiO_2 nanoparticles, aqueous solution of titanium (IV) isopropoxide was used as starting material. The sol was prepared by mixing titanium isopropoxide (3 ml) with 24 ml of ethanol and dissolved 1000 ml of doubly distilled water at room temperature. The molar ratio of titanium isopropoxide and alcohol is 1:8 respectively. Hydroxylamine hydrochloride 0.694 g was dissolved in 100 ml of deionised water and added gradually to the titanium isopropoxide sol. After stirring, an aqueous solution was centrifuged by using centrifuge machine. The precipitate obtained was dried at 105° C in hot air oven. It was then calcinated at 600° C in a muffle furnace for 5 h at a constant temperature rise of 2° C/minute. For the preparation of 1 wt %, 3 wt %, 5 wt % W-doped TiO_2 nanoparticles, aqueous solution of titanium (IV) isopropoxide was used as starting material. The sol was prepared by mixing titanium isopropoxide (3 ml) with 24 ml of ethanol and dissolved 1000 ml of double distilled water at room temperature. The molar ratio of titanium isopropoxide and alcohol is 1:8 respectively. Hydroxylamine hydrochloride 0.694 g was dissolved in 100 ml of deionised water and added gradually to the titanium isopropoxide sol. For tungsten doping 1 wt % of sodium tungstate dihydrate solution was added into the TiO_2 sol. The mixture of titanium (IV) isopropoxide and sodium tungstate dihydrate solutions were stirred for 3 h in the magnetic stirrer. After stirring, an aqueous solution was centrifuged by using centrifuge machine. The precipitate obtained was dried at 105° C in hot air oven. It was then calcinated at 600° C in a muffle furnace for 5 h at a constant temperature rise of 2° C/minute. Similarly 3 wt % and 5 wt % W-doped TiO_2 powders were prepared by the same procedure as mentioned in the above method.

2.3. Antimicrobial activity

2.3.1. Preparation of culture media

2.3.1.1 *Nutrient agar medium*

Nutrient agar medium of pH 7 is one of the most commonly used medium for several routine bacteriological purposes. It was prepared by dissolving 5 g of peptone, 3 g of beef extract, 15 g of agar, 5 g of sodium chloride, 1.5 g of yeast extract in 100 ml of distilled water, it is boiled to dissolve the medium completely and sterilized by autoclaving at 15 Ib psi pressure (121° C) for 15 min.

2.3.1.2 *Inoculum preparation*

Bacterial cultures were subcultured in liquid medium (Nutrient broth) at 37° C for 8 h and further used for the test (10^5-10^6 CFU /ml). The suspensions were prepared before the test was carried out.

2.3.1.3 *Assay of antimicrobial activity*

The nutrient broth was prepared, and bacterial and fungal colonies were inoculated into the broth culture and are used to assay the antimicrobial activity.

2.3.2 Inhibition zone assay (Kirby Bauer Agar Well Diffusion Assay)

The nutrient agar medium was prepared and sterilized by autoclaving at 121° C 15 lbs pressure for 15 min then aseptically poured the medium into the sterile petriplates and allowed to solidify the bacterial and fungal broth culture was swabbed on each petriplates using a sterile buds. Then, wells were made by well cutter. 1 wt %, 3 wt % and 5 wt % W-doped TiO_2 nanoparticles containing solutions were prepared dissolving 100 mg of each in 100 ml of DMSO solvent and from this stock solution, different concentrations of 1 wt %, 3 wt % and 5 wt % W-doped TiO_2 nanoparticles calcinated at 600° C (25 µg, 50 µg, 75 µg and 100 µg) solutions were taken for assay.

The antimicrobial activity of 1 wt %, 3 wt % and 5 wt % W-doped TiO_2 nanoparticles calcinated at 600° C were assayed against *Staphylococcus aureus, Bacillus subtilis, Escherichia coli, Pseudomonas aeruginosa, Aspergillus niger* and *Candida albicans* at 37° C for 24 h. After incubation the plates were observed for the zone of inhibition.

The bacterial and fungal viable count was determined after 24 h by plating pure TiO_2, 1 wt %, 3 wt % and 5 wt % W-doped TiO_2 nanoparticles calcinated at 600° C on nutrient agar plates and the number of colony forming units (CFU) which were counted by a viable count method. To control this, the bacterial and fungal cultures were incubated with Gentamicin. The sample material which has antimicrobial activity was identified by inhibited growth of the microorganisms and it is clearly seen as distinct zone of inhibition. The diameter of zone of inhibition was measured and expressed in millimetre [10]. The prepared 1 wt %, 3 wt % and 5 wt % W-doped TiO_2 nanoparticles calcinatedat 600° C nanoparticles with the sizes varied from 28 to 34 nm. Kirby Bauer Agar Well Diffusion Assay test was conducted using 1 wt %, 3 wt % and 5 wt % W-doped TiO_2 nanoparticles calcinated at 600° C nanoparticles and common antibiotic Gentamicin. The diameter of zone of inhibition for 1 wt %, 3 wt % and 5 wt % W-doped TiO_2 nanoparticles calcinated at 600° C was compared to this antimicrobial agent [11]. The diameter of zone of inhibition for pure TiO_2 at 600° C was also compared to this antimicrobial agent. To analyse the antimicrobial activity of 1 wt %, 3 wt % and 5 wt % W-doped TiO_2 nanoparticles calcinated at 600° C was obtained by the microemulsion method.

3. Results and discussion

3.1. X-ray diffraction analysis (XRD)

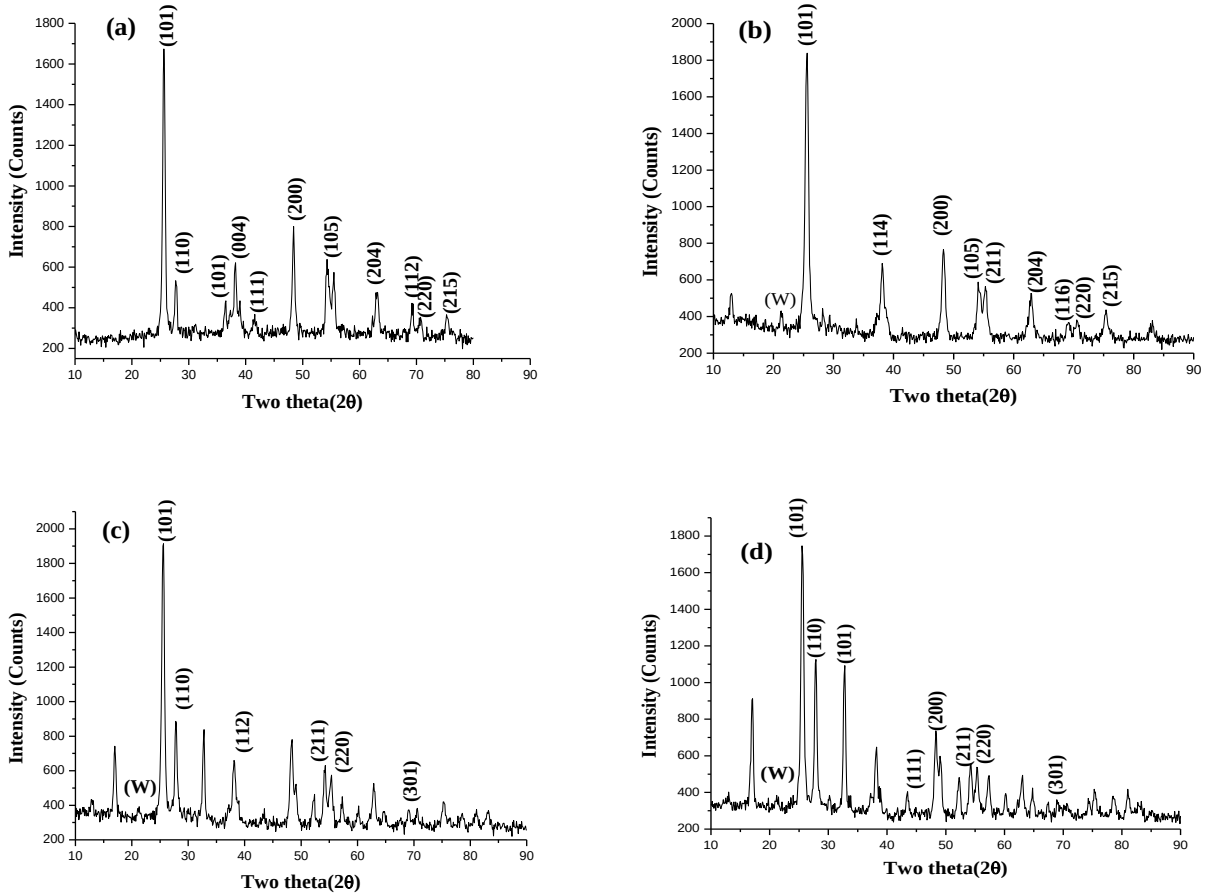

Figure 1 XRD pattern of (a) pure TiO_2 (b)1 wt % W-doped TiO_2 (c) 3 wt %W-doped TiO_2 and (d) 5 wt %W-doped TiO_2 calcinated at 600° C

X Ray Diffraction analysis was used to determine the crystalline structure and phase of the synthesised nanoparticles. Figure 1(a-d) shows the X Ray Diffraction patterns of pure and W-doped TiO_2 nanoparticles. The results shows that most of the peaks to pure and 1 wt % W-doped TiO_2 nanoparticles calcinated at 600° C confirms the formation of anatase phase by the existence of strong diffraction peaks at 2θ values of 25.3°, 38.44°, 48°, 54°, 55.07°, 63°, 69.23°, 70.89°, and 75.38° corresponding to the crystal planes of (101), (112), (200) (105), (211) (204), (116), (220), and (215), respectively [JCPDS card no 21-1272] belonging to the tetragonal structure. The XRD diffraction patterns obtained for 3 wt % and 5 wt % W-doped TiO_2 nanoparticles are shown in the Figure 1(c and d). It showed the presence of characteristic rutile peaks at 2θ values of 27.4°, 36.0°, 39.1°, 54.3°, and 64.0° 2□ to the crystal planes of (110), (101), (200), (211), and (002) respectively□ □(JCPDS: 88-1175) being a mix of anatase and rutile phase. The fineness peaks indicates that the nanosized materials were well crystallized. There are several studies reported [12, 13, 14] that sol-gel sample of TiO_2 should undergo a phase transformation from anatase to rutile during the higher calcinations (above 500° C) temperature in general. Here, the results showed that major phase transformation from anatase to rutile takesplace with the increase of wt % of WO_3, new peaks appeared at 2θ =20.45° and 22.83° (marked as W), for the W-doped TiO_2.The new peaks may be attributable to a new component of $W_xTi_{1-x}O_2$. It has been observed by other researchers that, At high wt % of tungsten doping (5 wt %), retarded the phase transformation (up to 900° C) [15, 7]. But this experiment is not found in any retardant at the current level of doping (3 wt % and 5 wt %) [16] is due to W ions in TiO_2 can either replace titanium ions to form W-O-Ti bonds or locate at interstitial sites.

The average particle size of pure TiO_2 is 37 nm and 1 wt %, 3 wt % and 5 wt % W-doped TiO_2 powders are about 28 nm, 34 nm and 33 nm respectively. The average particle sizes was calculated using the full-width at half maximum measurement at 2θ of the maximum diffraction peaks using the following Debye-Scherrer's formula,

$$D=K\,\lambda/\,\beta\cos\theta$$

In this equation, D is the crystallite size, K the Scherrer constant usually taken as 0.89, λ the wavelength of the X-ray radiation (0.15418nm for Cu Kα). Comparing the XRD patterns W-doped TiO_2, it appears that W loading does not influence the crystalline structure of TiO_2.

3.2. Field Emission Scanning Electron Microscope (FESEM)

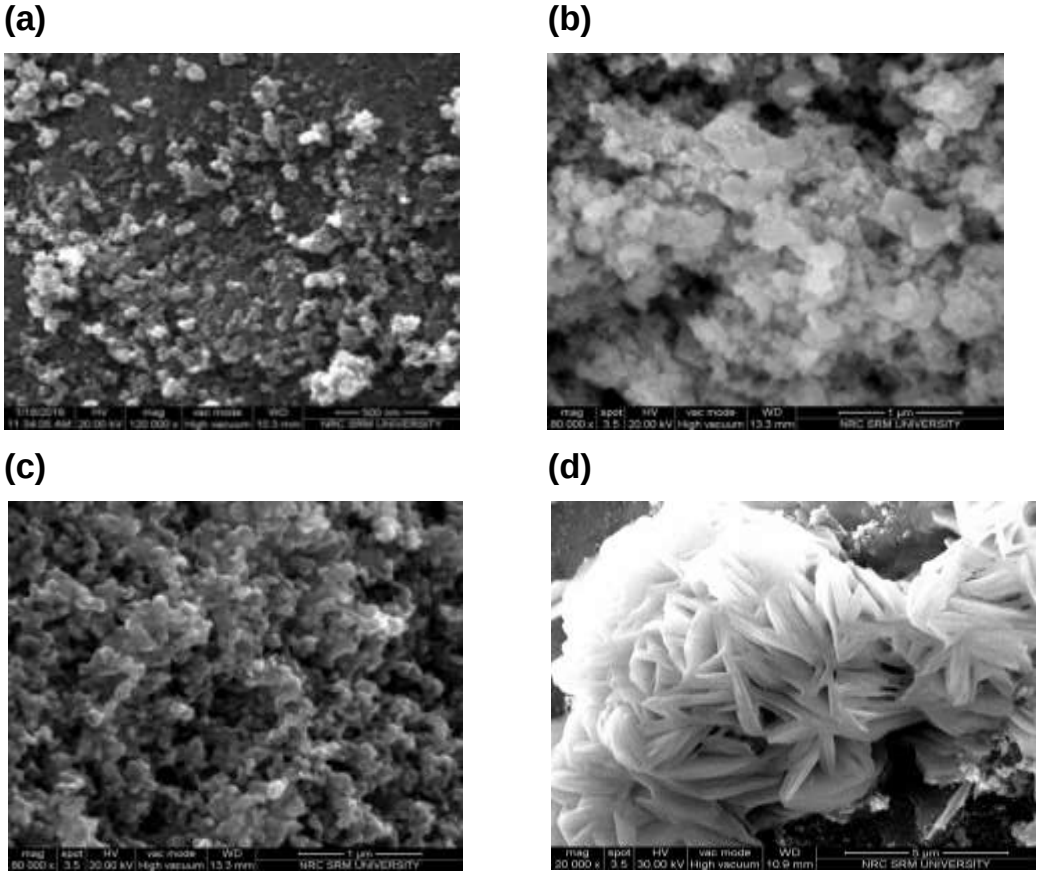

Figure 2 FESEM micrographs of (a) pure TiO_2 (b) 1 wt % W-doped TiO_2 (c) 3 wt % W-doped TiO_2 and (d) 5 wt % W-doped TiO_2 calcinated at 600° C

The FESEM images of pure and W-doped TiO_2 calcinated at 600° C are shown in Figure 2 (a-d). From the images, it can be confirmed that the average agglomerated particle size is nearly spherical and homogeneous particles. FESEM micrograph of W-doped TiO_2 nanoparticles shows that the surface morphology of the particles is nearly spherical with uniform sized particles and coherent together. However, the individual spherical particles are clearly seen due to the nano-clusters formed during the growth for 1 wt %, 3 wt % W-doped TiO_2. But it can be seen from the 5 wt % W-doped TiO_2 nanoparticles, nanorod type of nanoparticles were obtained. It can be seen that the average agglomerated particle size of 1 wt%, 3 wt % W-doped TiO_2 prepared by sol-gel method has no influence on the particle except 5 wt % W-doped TiO_2.

3.3. Energy Dispersive Analysis by X-Rays (EDXA)

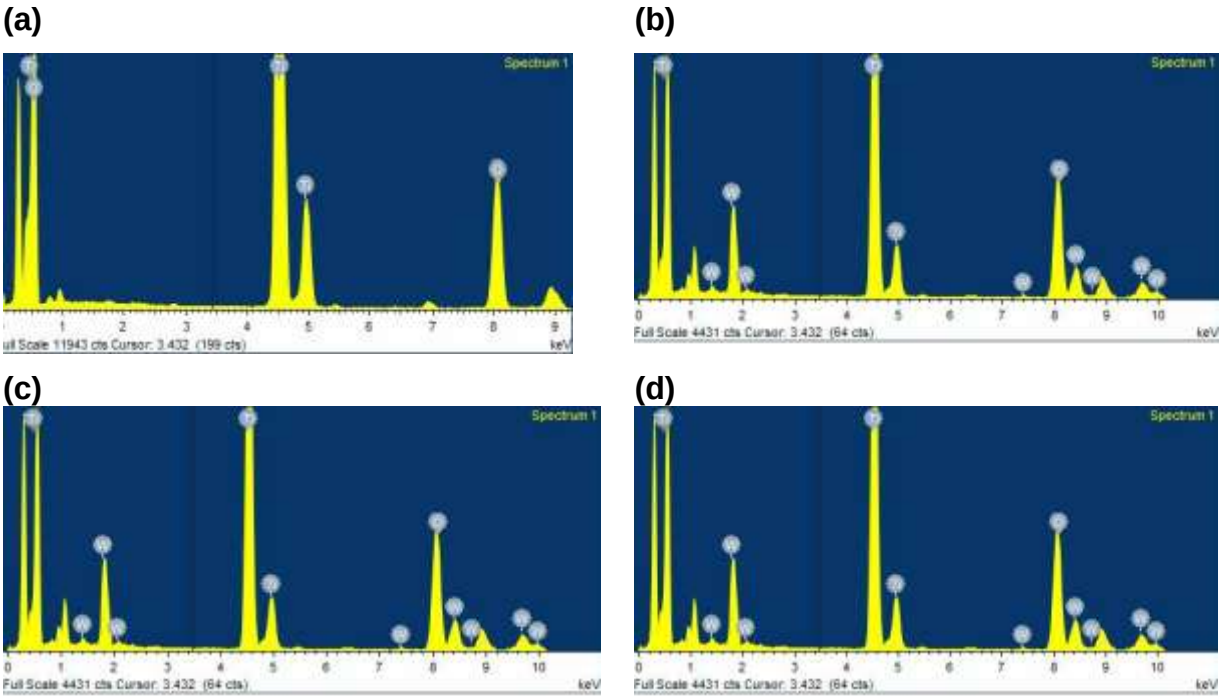

Figure 3 EDXA pattern of pure, 1 wt %, 3 wt % and 5 wt % W-doped TiO_2 nanoparticles calcinated at 600° C

Analysis of EDXA is used to analyze the chemical composition of the prepared material. It is clear that from the figure 3(a) TiO_2 is in pure form and free from any observable impurities. Figure 3 (b-d) also shows the EDXA of 1 wt %, 3 wt % and 5 wt % W-doped TiO_2 samples, prepared by sol-gel method. EDXA shows only peaks of titanium, tungsten and oxygen elements. From the figure, it is clear that W-doped TiO_2 is free from impurities.

3.4. UV–Visible diffuse reflectance spectra (UV-Visible spectra)

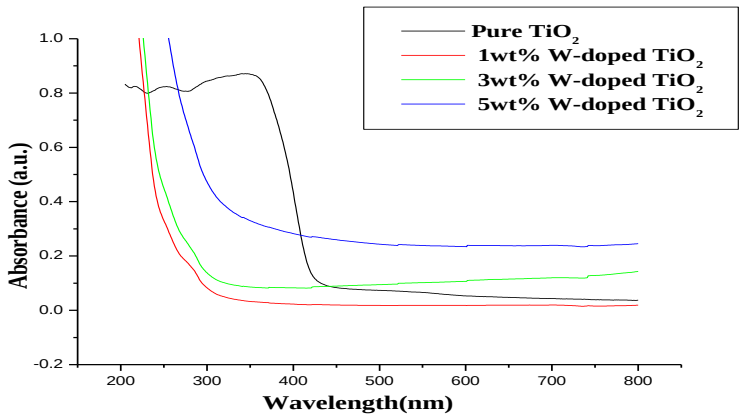

Figure 4 UV-Vis diffuse reflectance spectra of pure TiO_2, 1 wt %, 3 wt % and 5 wt % of W-doped TiO_2 calcinated at 600° C

UV-Visible spectroscopy measurement was performed to explore the absorbance and band gap of pure and 1 wt %, 3 wt % and 5 wt % W-doped TiO_2 nanoparticles. The optical absorbance spectra of pure and W-doped TiO_2 samples were recorded by a UV-Vis spectrophotometer in the range of 200-800 nm are shown in figure 4. From the figure, it indicates that blue shift was observed for pure TiO_2 compared with W-doped TiO_2 samples. The band edge absorption for pure TiO_2 blue shifted with tungsten doping indicates that widening of the optical band gap of pure TiO_2 [17]. The obtained results can be confirms the band gap value of W-doped TiO_2 (4.47 eV, 3.96 eV and 3.41 eV) larger than the pure TiO_2 (2.86 eV).

But in the case of UV-Vis absorbance spectra of doped TiO_2, 1 wt %W-doped TiO_2 compared with other doped (3 wt % and 5 wt %) TiO_2 samples observed redshift when increasing the doping concentration of tungsten. It can be seen that from the figure 4. Optical absorption edges are shifted to higher wavelength region (red shift) with increasing dopant tungsten [18]. This redshift may create consistent of the tungsten onto the TiO_2 crystal lattice which creates impurity in the band gap [19] leading to reduction in the band gap energies [20]. The band gap of the samples can be determined by extrapolation of the absorption edge onto the x-axis and using the Planck's equation

$$E_g=hC/\lambda$$

Where E_g is the energy gap of pure and dopedTiO_2 at absorption wavelength λ,

h is the Planck's constant,

C is the velocity of light

The calculated bandgap values for pure TiO_2 is 2.86 eV and W-doped nanoparticles values are 4.47 eV, 3.96 eV and 3.41 eV. From the bandgap values of W-doping, decreases when increase the doping of W content which shift to the longer wavelength. This may be attributed to the new electronic states and are introduced in the middle of the TiO_2 bandgap after doping the W atoms [18].

3.5 Photoluminescence study (PL)

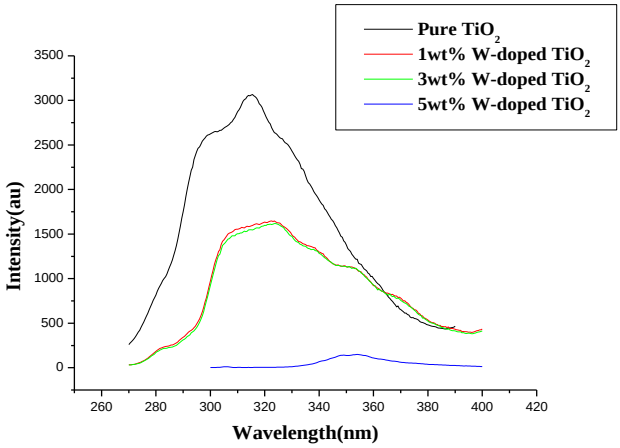

Figure 5 Photoluminescence spectrum of pure TiO_2, 1 wt %, 3 wt % and 5wt % W-doped TiO_2 samples calcinated at 600° C

Photoluminescence spectroscopy (PL) is a useful method to find the efficiency of trapping of charge carrier, transfer and circumstances of electron-hole pairs in semiconductor particles. The excitation wavelength of the pure TiO_2 is found to be at 325 nm. Similarly, for other excitation wavelength of W-doped TiO_2 nanoparticles is observed at 325 nm, 325 nm and 355 nm which indicates that trapped electrons and oxygen vacancies. Photoluminescence spectra of pure TiO_2 is greater than the PL intensity of 1 wt %, 3 wt % and 5 wt % W-doped TiO_2, which is due to a lower recombination rate of electrons and holes [21, 22] in the presence of light irradiation by the transition of energy levels between WO_3 orbital and TiO_2 orbital. It takesplace by photogenerated electrons and are transferred to WO_3 conduction band from TiO_2 conduction band and the holes accumulate in the TiO_2 valence band which results in photogenerated electrons and holes are separated. The figure 5 shows the photoluminescence spectrum of pure and 1 wt %, 3 wt % and 5 wt % W-doped TiO_2 nanoparticles which show that the position of the peaks is almost similar except the 5 wt % W-doped TiO_2 nanoparticles and the photoluminescence intensity of pure TiO_2 is greater than the PL intensity of W-doped TiO_2. It indicates that the recombination of charge carriers is effectively reduced by the doping tungsten metal [23]. The peaks for the doped TiO_2 shift to red direction and also this shift of emission peak towards longer wavelengths further supports the lowering of the band gap of TiO_2 due to the tungsten doping treatment.

3.6 Fourier Transform Infrared Spectroscopy (FTIR)

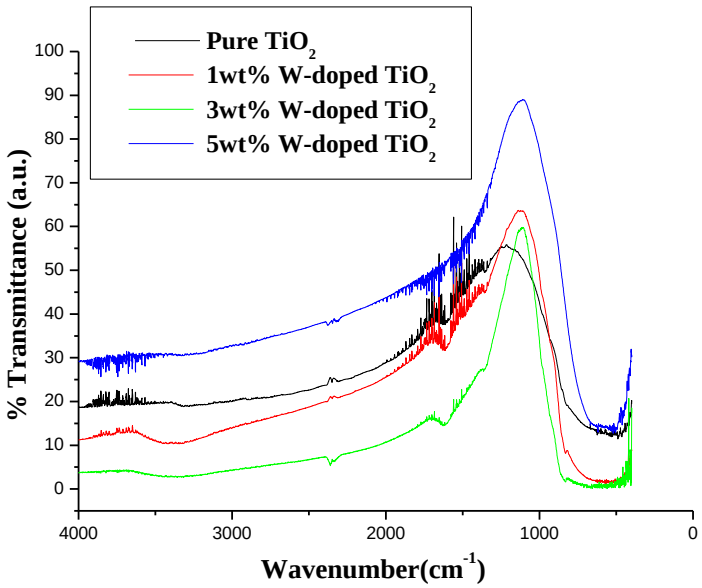

Figure 6 Fourier transforms infrared spectra of (a) pure TiO_2, (b) 1 wt % W-doped TiO_2, (c) 3 wt % W-doped

TiO_2 and (d) 5 wt % W-doped TiO_2 samples calcinated at 600° C

IR spectra of pure and W-doped TiO_2 are shown in Figure 6. The absorption bands are shown in the region of 3300-3400 cm^{-1} for vibrations of O-H and 1620-1630 cm^{-1} in the region indicates the bending vibrations of the molecules. The little difference of band around 450 to 800 cm^{-1} indicates the presence of Ti-O-W, compared to pure TiO_2 [24].

3.7 High Resolution Transmission Electron Microscopy (HRTEM)

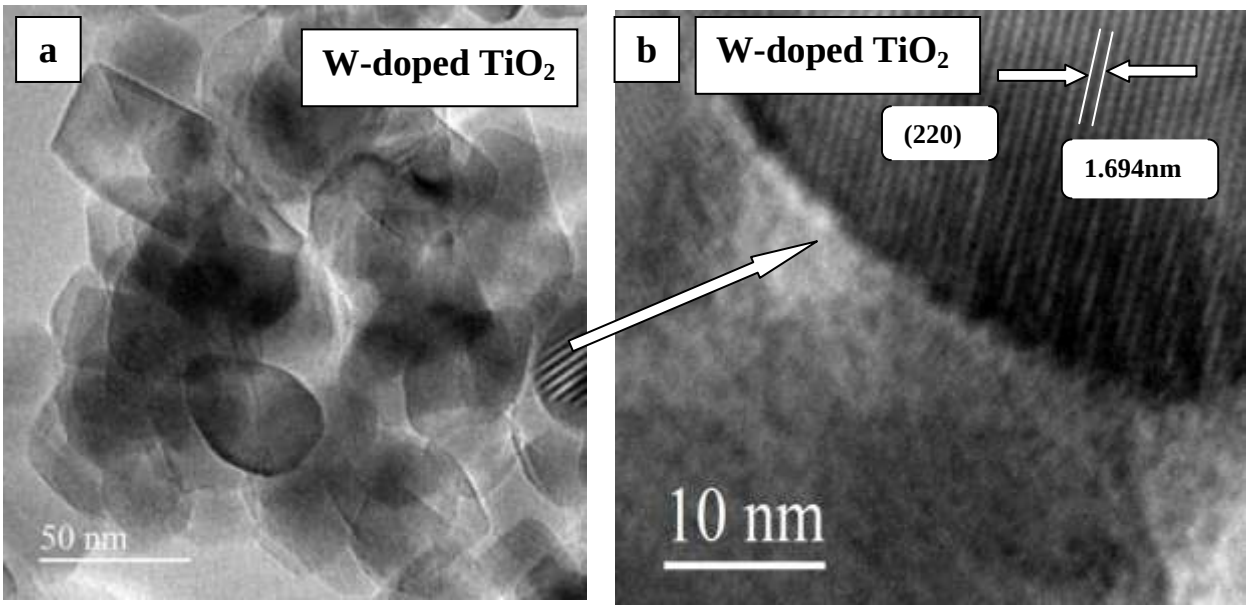

Figure 7 High Resolution Transmission Electron Microscopy image of W-doped TiO_2

The High Resolution TEM is used to study the morphology, distribution pattern, growth, of sample and it is also used to confirm the size of the particles. From the images clearly confirms that particles present in the W-doped TiO_2 powdered sample is nanosized particles. HRTEM images shows, all the particles are in irregular shapes and agglomerated. The figure (b) shows presence of fringes which are identified by lattice d-spacing values of 1.694 nm which correspond to the lattice spacing values (220) by using the standard JCPDS data.

3.8 Antimicrobial activity

(a) Staphylococcus aureus (Gram positive)

Pure TiO_2 calcinated at 600° C | 1 wt % W-doped TiO_2 | 3 wt % W-doped TiO_2 | 5 wt % W-doped TiO_2

(b)Bacillus subtilis (Gram positive)

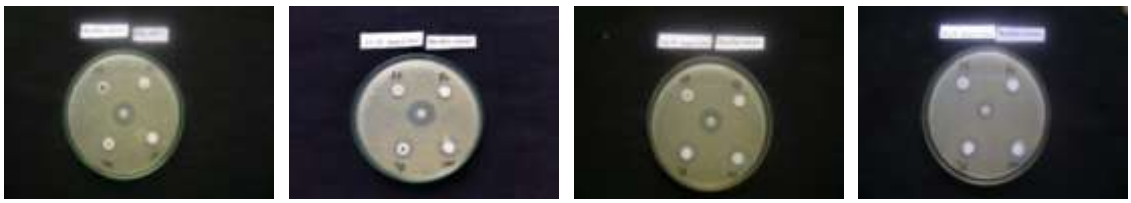

Pure TiO_2 calcinated at 600° C | 1 wt % W-doped TiO_2 | 3 wt % W-doped TiO_2 | 5 wt % W-doped TiO_2

(c) Escherichia coli (Gram negative)

Pure TiO_2 calcinated at 600° C | 1 wt % W-doped TiO_2 | 3 wt % W-doped TiO_2 | 5 wt % W-doped TiO_2

(d) Pseudomonas aeruginosa (Gram negative)

Pure TiO_2 calcinated at 600° C | 1 wt % W-doped TiO_2 | 3 wt % W-doped TiO_2 | 5 wt % W-doped TiO_2

(e)Candida albicans (fungus)

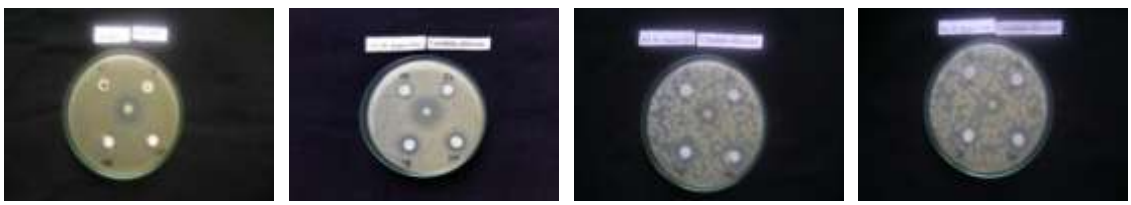

Pure TiO_2 calcinated at 600° C | 1 wt % W-doped TiO_2 | 3 wt % W-doped TiO_2 | 5 wt % W-doped TiO_2

(f) Aspergillus niger *(fungus)*

ISSN 2321-807X
Volume 13 Number3
Journal of Advances in chemistry

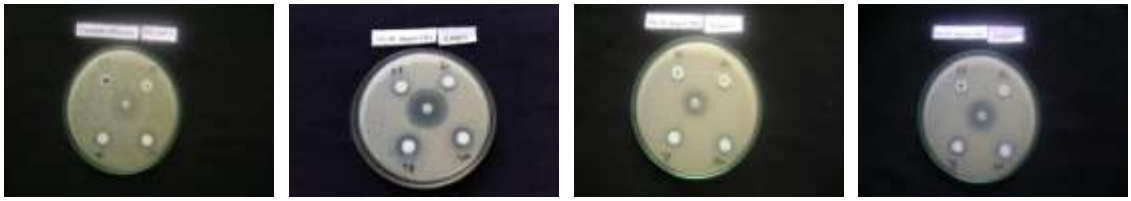

Pure TiO_2 calcinated at 600° C | 1 wt % W-doped TiO_2 | 3 wt % W-doped TiO_2 | 5 wt % W-doped TiO_2

Figure 7(a-f) Inhibition zone of different microorganism by media s subjected to pure TiO_2, 1 wt % W-doped TiO_2, 3 wt % W-doped TiO_2, 5 wt % W-doped TiO_2 calcinated at 600° C

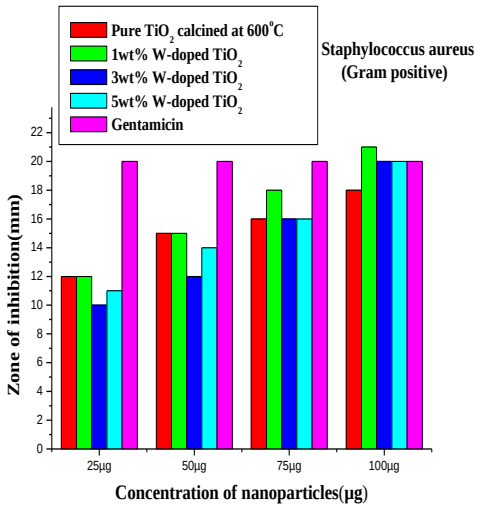

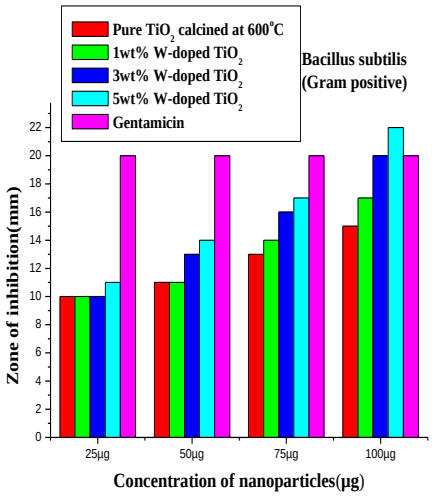

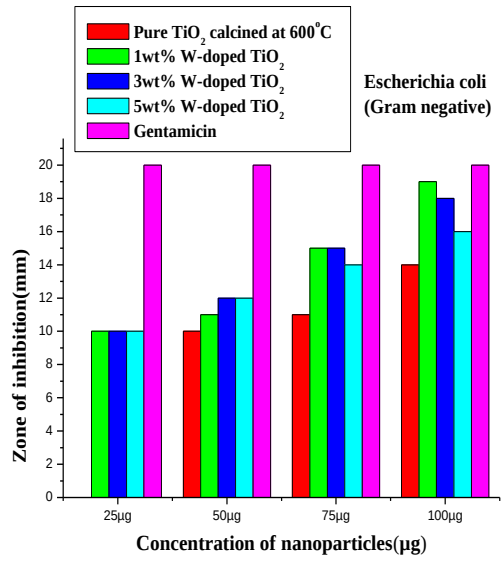

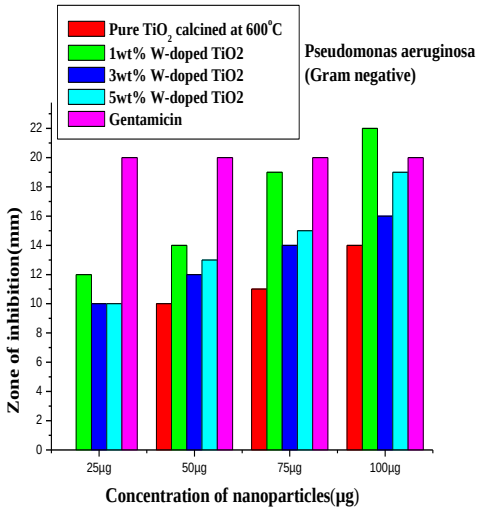

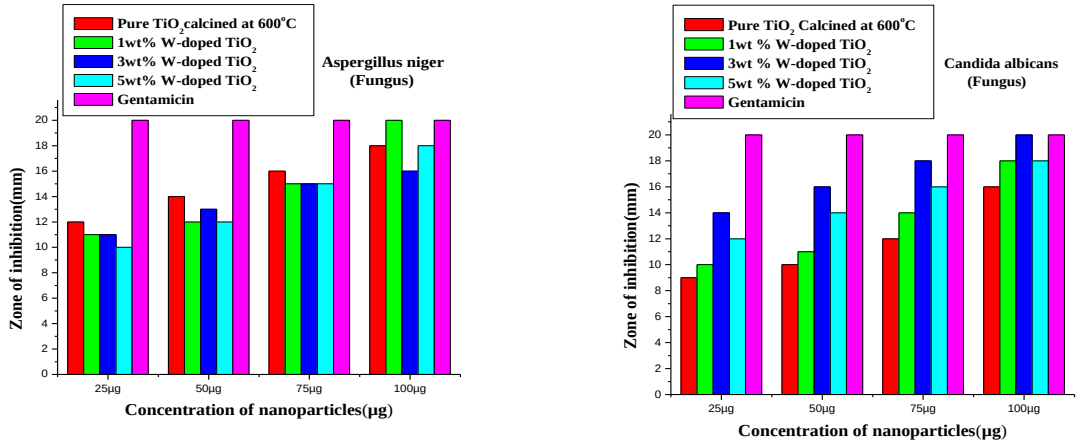

Figure 8 Antibacterial effects of pure TiO_2, 1 wt % W-doped TiO_2, 3 wt % W-doped TiO_2, and 5 wt % W-doped TiO_2 calcinated at 600° C

The antimicrobial activities of the samples are identified from the zone of inhibition. The diameter of zone of inhibition was measured and expressed in millimeter. The results showed that for all of the four samples at different concentration showed some good zone of inhibition against all the pathogens used. In addition, it could be observed that the doped samples are having much higher zone of inhibition compared to the pure TiO_2 sample. It shows that there is a significant effect of the tungsten induced antimicrobial activity for all the other doped samples. Also, the zone of inhibition increases as the concentration of the samples increases for almost all the samples against all the pathogens. However, none of the samples were able to reach the zone of inhibition of the standard Gentamicin except for the two samples which showed some higher zone of inhibition against the gram positive bacteria. The 1 wt % W-doped TiO_2 at higher concentration (100 mg) showed a higher zone of inhibition against the gram positive bacteria *Staphylococcus aureus* compared to all other pure and doped samples. However the 3 wt % and 5 wt % W-doped TiO_2 showed the zone of inhibition to that of the standard Gentamicin. Similar results were observed for the 3 wt % W-doped TiO_2 against the gram positive bacteria *Bacillus subtilis*.1 wt % W-doped TiO_2 at higher concentration showed a higher zone of inhibition compared to the standard Gentamicin against the gram negative bacteria *Pseudomonas aeruginosa*. These results proved that the effect of the W doping on TiO_2 enhances the antimicrobial activity due to modified surface area, morphology and the reactivity of the samples.

CONCLUSION

Pure and 1 wt %, 3 wt % and 5 wt % W-doped TiO_2 nanoparticles were successfully synthesized by sol-gel method using hydroxylamine hydrochloride as a hydrolysis catalyst. The prepared nanoparticles are calcinated at 600° C for 5 h. According to the XRD pattern, 1 wt % W-doped TiO_2 was in an anatase crystalline form and it may be due to the smaller amount of W in TiO_2. It did not affect the crystalline structure. Whereas 3 wt % and 5 wt % W-doped TiO_2 shows rutile crystalline structure which confirms the phase transformation due to the tungsten doping. The average particle sizes of pure TiO_2 powder is approximately 37 nm. The average particle size of 1 wt %, 3 wt %, and 5 wt % W-TiO_2 powders are about 28 nm, 34 nm and 33 nm respectively. FESEM images of 1 wt % 3 wt % and 5 wt % W-doped TiO_2 which confirms the spherical with uniform sized particles and coherent together of all these nanoparticles. EDXA analysis shows that no impurities were present in the prepared pure and W-doped samples. UV-Vis absorbance spectra of doped TiO_2, 1 wt % W-doped TiO_2 compared with other doped 3 wt % and 5 wt % TiO_2 samples observed redshift when increasing the doping concentration of tungsten The bandgap values of W-doping, decreases when increase in the doping of W content which shift to the longer wavelength. This may be attributed to the new electronic states and are introduced in the middle of the TiO_2 bandgap after doping the W atoms PL spectrum indicates that the recombination of charge carriers is effectively reduced by the doping tungsten metal. From the HRTEM images spherical shaped particles are shown. But all the spherical shaped nanoparticles are agglomerated together to form a larger particle present in the nanostructure domain and particles size are approximately 30 to 35. Broadening of peak of pure TiO_2 in FTIR spectra is due to increasing the W doping. Antibacterial activity of the W doping on TiO_2 enhances the antimicrobial activity due to modified surface area, morphology and the reactivity of the samples.

References

[1].M.R. Hoffmann, S.T. Martins, W. Choi, D.W. Bahnemann, Environmental Applications of Semiconductor Photocatalysis Chem. Rev. 95 (1995) 69–96.

[2].A. Fujishima, T.N. Rao, D.A. Tryk, Titanium dioxide photocatalysis, J. Photochem. Photobiol. C. 1 (2000) 1.

[3].Rajeshwar K, J. Appl. Electrochem .Photoelectrochemistry and the environment,

25 (1995)1067–1082.

[4].S.D. Mo, W.Y. Ching, Phys. Rev. B Electronic and optical properties of three phases of titanium dioxide: Rutile, anatase, and brookite 51-19 (1995)13023.

[5].T. Putta, M.C. Lu, J. Anotai, Photocatalytic activity of tungsten-doped TiO_2 with hydrothermal treatment under blue light irradiation, J. Environ. Manag. 92,(2011) 2272– 2276.

[6]. G. Ramis, G. Busca, C. Cristiani, L. Lietti, P. Forzatti, F. Bregani, Characterization of tungsta-titania catalysts Langmuir 8, (1992)1744– 1749.

[7].V.Stengl, J. Velicka, M. Marikova, T.M. Grygar, New Generation Photocatalysts: How Tungsten Influences the Nanostructure and Photocatalytic Activity of TiO_2 in the UV and Visible Regions,ACS Appl. Mater. Interfaces 3, (2011)4014–4023.

[8].H. Yang, D. Zhang, L. Wang, Synthesis and characterization of tungsten oxide-doped titania nanocrystallites Mater. Lett. 57,(2002) 674–678.

[9].D.Byun, Y.Kim, K.Lee, P.Hofmann, Photocatalytic TiO_2 deposition by chemical vapor deposition, Journal of Hazardous Materials, 73(2) (2000) 199-206.

[10].A.W.Bauer, M.M. Kirby,J.C. Sherris, M.Truck Antibiotic susceptibility testing by a standardized single disk method. Am J ClinPathol 45(1966) 493–496.

[11]. Zieli'nska A, Kowalska E, Sobczak JW, Łacka I, Gazda M, Ohtani B et al Silver-doped TiO_2 prepared by microemulsion method: surface properties, bio- and photoactivity. Sep Purif Tech 72(2010) 309–318.

[12].T.V.L Thejaswini, N. Saraschandra, D. Prabhakaran, V.K. Indira Priyadharshini, Evaluation of Photocatalytic Activity of Ag I and Sr II co-doped TiO_2 Nanoparticles for the Degradation of Reactive Blue-160 (RB-160) Textile Dye. International Journal of Advanced Chemical Science and Applications. Volume -2, Issue -2, (2014) 35-41.

[13]. A. Linsebigler, G. Lu, J.T. Yates, Photocatalysis on TiO_2 Surfaces: Principles, Mechanisms, and Selected Results Chem. Rev. 95 (1995) 735.

[14]. Engweiler, J. Harf, A.Baiker, WOx/TiO_2Catalysts Prepared by Grafting of Tungsten Alkoxides: Morphological Properties and Catalytic Behavior in the Selective Reduction of NO by NH_3 J. Catal.159 (1996)259.

[15].S. Eibl, B.C. Gates, H. Knozinger, Structure of WO_x/TiO_2 Catalysts Prepared from HydrousTitanium Oxide Hydroxide: Influence of Preparation Parameters. Langmuir 17,(2001) 107– 115.

[16].S.A.K. Leghari, S. Sajjad, F. Chen, J.L. Zhang, WO_3/TiO_2 composite with morphology change via hydrothermal template-free route as an efficient visible light photocatalyst. Chem. Eng. J. 166,(2011) 906–915.

[17].P.S.Archana, Arunava Gupta, M.Mashitah. Yusoff and Rajan Jose, Tungsten doped titanium dioxide nanowires for high efficiency dye-sensitized solar cells.

[18]. Song, H. Jiang, H. Liu, X. Meng, G. J.Photochem. Photobiol, *A,* 2006, *181*, 421- 428.

[19].W.Choi, A.Termin, M.R.Hoffmann, M. R. *J. Phys. Chem.* 1994, *98*, 13669-13679.

[20].EkemenaOghenovohOseghea, Patrick GathuraNdungub, Sreekantha Babu Jonnalagaddaa, Photocatalytic degradation of 4-chloro-2-methylphenoxyacetic acid using W-doped TiO_2.

[21].S. Hu, F. Li and Z. Fan, Convenient Method to Prepare Ag Deposited N-TiO_2 Composite Nanoparticles *via* NH_3 Plasma Treatment. Bull. Korean Chem. Soc. 33 (2012) 2309–2314.

[22].Y. L. Kuo, H. W. Chen and Y. Ku, Analysis of silver particles incorporated on TiO_2 coatings for the photo decomposition of o-cresol.Thin Solid Films.515 (2007) 3461– 3468.

[23].R.Velmurugan, B. Krishnakumar, B. Subashand, M. Swaminathan, Preparation and characterization of carbon nanoparticles loaded TiO_2 and its catalytic activity driven by natural sunlight. Solar Energy Materials & Solar Cells.108 (2013) 205-212.

[24].Xue Li, Yunyi Liu, Pengfei Yang, YongchaoShi College of Chemical Engineering, Shenyang University of Chemical Technology, Shenyang, Visible light-driven photocatalysis of W, N co-doped TiO2 110142, Chinaa- Particuology.